

Computational Capacity of an Odorant Discriminator: the Linear Separability of Curves

N. Caticha* , J. E. Palo Tejada* , D. Lancet[◊] and E. Domany[#]

*Instituto de Física, Universidade de São Paulo, CP66318,
CEP 05315-970, São Paulo, SP, Brazil

#Department of Complex Systems,
Weizmann Institute of Science, Rehovot 76100, Israel

◊Department of Membrane Research and Biophysics,
Weizmann Institute of Science, Rehovot 76100, Israel

(August 2000)

We introduce and study an artificial neural network, inspired by the probabilistic Receptor Affinity Distribution model of olfaction. Our system consists on N sensory neurons whose outputs converge on a single processing linear threshold element. The system's aim is to model discrimination of a single target odorant from a large number p of background odorants, within a range of odorant concentrations. We show that this is possible provided p does not exceed a critical value p_c , and calculate the critical capacity $\alpha_c = p_c/N$. The critical capacity depends on the range of concentrations in which the discrimination is to be accomplished. If the olfactory bulb may be thought of as a collection of such processing elements, each responsible for the discrimination of a single odorant, our study provides a quantitative analysis of the potential computational properties of the olfactory bulb. The mathematical formulation of the problem we consider is one of determining the capacity for linear separability of continuous curves, embedded in a large dimensional space. This is accomplished here by a numerical study, using a method that signals whether the discrimination task is realizable or not, together with a finite size scaling analysis.

I. INTRODUCTION

The basic machinery for olfaction, our ability to smell, is an array of a few hundred different types of sensory neurons. Each of these expresses molecular receptors, that belong to a single type. When this small neuronal assembly is exposed to external stimuli, its cooperative response is capable to detect and recognize a wide variety of *odorants* and to measure their concentrations. We use the terminology "odorant" to describe any chemically homogenous substance (ligand) which elicits a response from the olfactory system.

The response of the array of neurons to any particular odorant is determined by the responses of the individual constituent neurons. This response is, however, governed by the extent to which the receptors expressed by the particular neuron bind the odorant, i.e. by the *affinity* K of the neuron's receptors to the odorant. According to a recently proposed model [1], these affinities can be viewed as independent random variables, drawn from a single receptor affinity distribution (RAD), denoted by $\psi(K)$. Once a set of affinities (for all odorants and all sensory neurons) has been generated, the response of the entire sensory assembly to any odorant is determined.

This information is transferred from the sensory neurons to the olfactory bulb, onto which the axons of the sensory neurons project. They form synapses on secondary neurons (mitral and tufted cells). This integration of the sensory input, that takes place in the olfactory bulb, forms the first step of the information processing that takes place in the olfactory pathway. Interneurons of two major types (periglomerular and granule cells) are believed to play a role in computing the pattern transmitted from the olfactory bulb to higher brain centers.

In this paper we evaluate, on the basis of a very simple model, some of the potential computational characteristics of the olfactory bulb, as it performs this initial integration. We hope some of our quantitative results could be biologically relevant. Our simple model for the sensory array and a single processing unit is depicted in Fig. 1.

The model we introduce is, however, interesting also from a mathematical point of view. The problem of Linear Separability (**LS**) of points in N dimensional space has received considerable attention since the 19th century [2]. In the mathematics literature Cover studied the problem of **LS** of independent dichotomies using combinatorial methods [10]. In computer science the perceptron, introduced by Rosenblatt [8] and analyzed in detail by Minsky and Papert [11], gave a major boost to the field of neural networks. More recently, by introducing Statistical Mechanics techniques Gardner [3] extended Cover's results to cases where there are correlations between the points that have to be linearly separated.

We generalize the problem of separating (zero-dimensional) *points*, to the separability of (one-dimensional) *strings* or *curves*, embedded in N -dimensional space. In the context of our problem the curves that need be separated are parametrized continuously by the odorant concentration.

In principle one can address the separability of curves by placing a discrete set of points on each curve, thereby mapping the problem onto the previously solved one, of separating points. One should note, however, that points that lie on the same curve are not independent; in fact they are correlated in ways that render the previously developed analytical methods unapplicable. Therefore we present an extensive numerical analysis of the capacity of this special neural network, of N sensory neurons that provide input to a single processing unit. The capacity we calculate is interpreted as follows. The sensory system is exposed to $p + 1$ odorants, *one at a time*. One of these is the “target”; the aim is to distinguish the target from all the other $p = \alpha N$ odorants that form a “noisy olfactory background”.

The model, based on a single layer perceptron, is introduced and discussed in detail in section 2.1. Then we turn to describe the method we have developed in order to determine numerically the capacity. To do this we had to adapt and use several different techniques. One of these, a learning algorithm introduced by Nabutovsky and Domany [5], is described in Sec 2.2. This algorithm, like all other perceptron learning rules, finds the separation plane (if the problem *is LS*); however, unlike other learning algorithms, it provides a rigorous signal to the fact that a sample of examples is *not LS*.

Another technique we had to adapt to our purposes is finite size scaling (FSS) analysis of the data. The main results are presented in Sec 3 as curves of capacity as a function of odorant concentration in the thermodynamic ($N \rightarrow \infty$) limit, obtained by extrapolation, using FSS, from data obtained at a sequence of N values. This large N limit is quite natural from both practical and theoretical points of view. In practice, for N of the order of a few hundred, the results can hardly be distinguished numerically from those at the $N \rightarrow \infty$ limit. As to the theoretical side, the situation in this limit is much cleaner and easier to analyze. The final section 4 contains a critical discussion of the results from a biological point of view.

Our central finding is summarized in Fig 6; if we fix the range of concentrations in which the system operates, and increase the number of background odorants, we will reach a critical number p_c beyond which the system fails to discriminate the target. This critical number is proportional to the number of sensory neurons N , i.e. $p_c = \alpha_c N$, and it decreases when the concentration range increases.

II. COMPUTATIONAL MODEL

A. Odorant identification as Linear Separation of Curves in N-dimensional space

The simple neural assembly that is considered here consists of a single secondary neuron, which receives inputs from an array of N units that model the sensory neurons. The single secondary neuron represents a “grandmother cell”, whose task is to detect one particular “target” odorant, labeled 0. The sensory scenario we consider allows exposure of the neuronal assembly to a single odorant, which may either be the target odorant or one of $p = \alpha N$ background odorants. The odorant provides simultaneous stimuli to the N sensory neurons. The aim of the single secondary neuron is to determine whether the odorant that generated the incoming signal from the sensory array is the target odorant 0 or not. We assume that all odorants, background and target, are presented to the sensory array in concentrations H that lie within a range

$$H_{min} < H < H_{max} \quad (1)$$

We pose the following, well defined quantitative question:

What is the maximal number p_c of different background odorants that our neuron can distinguish from the target, for any concentration within the prescribed range ?

To sharpen the question, we put it in a more precise mathematical form. Consider $\mu = 1, 2, \dots, p$ background odorants with respective concentrations H^μ in the range (1). Odorant μ is characterized by the $i = 1, \dots, N$ affinities K_i^μ of the N receptors. According to the RAD model, these affinities are selected independently from a distribution $\psi(K)$ [1].

All our numerical results were obtained using for $\psi(K)$ the form (note: $K \geq 0$)

$$\tilde{\psi}(K) = \frac{K}{\sigma^2} \exp\left(-\frac{K^2}{2\sigma^2}\right) \quad (2)$$

The average and variance of this distribution are given by

$$\langle K \rangle = \sqrt{\frac{\pi}{2}}\sigma \quad \text{var}(\tilde{\psi}(K)) = 0.65\sigma \quad (3)$$

The distributions suggested in [1] were Poisson and binomial. With regard to the computational limitations of our model, the important idea behind the RAD model lies not in the exact form of the distribution, but on the fact that the affinities can be thought of as independent random variables. The main computational features of our model will not be altered as long as the distribution has the following features: it is zero for negative affinities and it has finite first and second moments. We have used $\tilde{\psi}(K)$ since it satisfies the previous constraints and is easier to deal with in analytical calculations.

When receptor i is exposed to odorant μ , at concentration H^μ , its response is given by

$$S_i^\mu = f(K_i^\mu H^\mu) \quad (4)$$

where $f(x)$ is a sigmoid shaped function; we use

$$f = x/(1+x) \quad (5)$$

throughout this paper.

The value taken by the affinity K_i^μ sets the particular concentration scale at which odorant μ affects the i th sensory neuron. From this point on we set $\sigma = 1$ in eq. (2); this means that the concentrations are measured in inverse units of the parameter σ .

The set of values $\{S_i^\mu\} = \{S_1^\mu, S_2^\mu, \dots, S_N^\mu\}$ constitute a vector of signals \mathbf{S}^μ , generated by the entire sensory array, when it is exposed to odorant μ . The $\{S_i^\mu\}$ serve as inputs to our secondary neuron, which we model as a linear threshold element or perceptron; its output signal is given by

$$s^\mu = \text{sign} \left(\sum_i^N w_i S_i^\mu \right) = \text{sign} (\mathbf{w} \cdot \mathbf{S}^\mu) \quad (6)$$

The simple neural network described above is schematically presented in Fig. 1. The sensory neurons are represented by boxes and the secondary neuron by a circle.

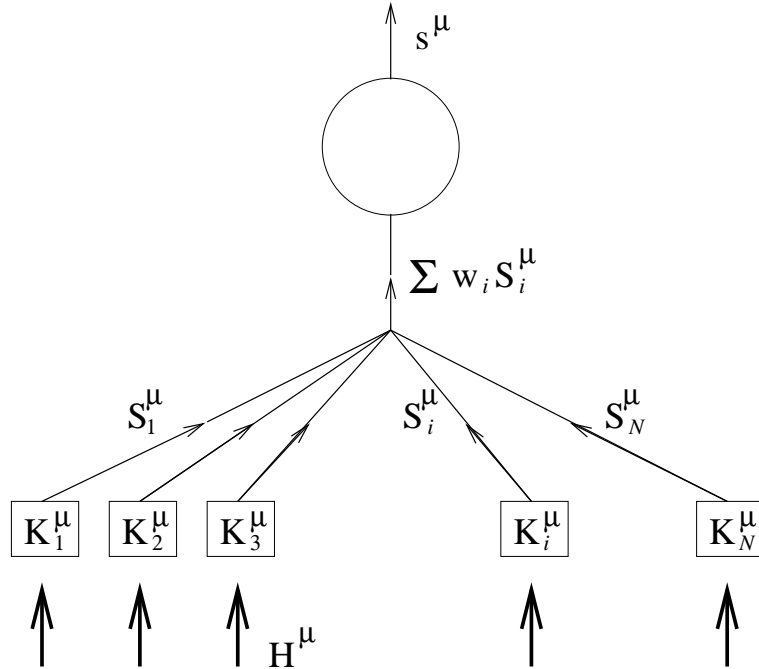


FIG. 1. Schematic representation of our model. N sensory neurons, represented by boxes, are exposed to odorant μ , present in concentration H^μ . Each sensory neuron i is characterized by a set of affinities K_i^μ ; the sensory input elicits from neuron i a response S_i^μ , as given by eq. (4,5). A weighted sum of the N sensory responses serves as the input of the secondary neuron (circle), whose output s^μ , generated in response to odorant μ , is given by eq. (6).

We require the output of this neuron to differentiate the target odorant from the background, i.e. yield

$$s^\mu = \begin{cases} -1 & \text{for } \mu = 1, \dots, p \text{ (background)} \\ +1 & \text{for } \mu = 0 \text{ (target)} \end{cases} \quad (7)$$

for **any** odorant concentration in the allowed range (1).

To understand the geometrical meaning of this requirement, note that when the concentration of odorant μ is varied in the allowed range (1), the corresponding vector \mathbf{S}^μ traces a *curve* (or *string*) in the N -dimensional space of sensory responses. The requirement (7) means that there exists a hyperplane, such that the entire curve that corresponds to the target odorant lies on one side of it, while the curves that correspond to *all* p background odorants lie on the other side. This explains our statement, made in the Introduction, that the problem we solve deals with the *Linear Separability of curves*.

We show that a solution to this classification problem can be found, provided $p < p_{max} = \alpha_c N$. We estimate the critical capacity α_c numerically. This is done by extrapolating results obtained for various values of N , using finite size scaling techniques, to the limit $N \rightarrow \infty$. The value of α_c is evaluated as a function of the limiting odorant concentrations.

In order to obtain these results using existing methodology, the most natural and straightforward thing to do is to place a discrete set of $\zeta = 1, 2, \dots, M$ points $\mathbf{S}^{\mu\zeta}$ on each curve, corresponding to different concentrations, and to require that the M points that lie on the curve of the target odorant are linearly separable from the PM points that represent the background. That is, equations (7) become

$$s^{\mu\zeta} = \begin{cases} -1 & \text{for } \mu = 1, \dots, p; \quad \zeta = 1, \dots, M \text{ (background)} \\ +1 & \text{for } \mu = 0; \quad \zeta = 1, \dots, M \text{ (target)} \end{cases} \quad (8)$$

This raises the technical question of how many (discrete) representatives of the same odorant should be included in the learning set. We show below, that while the critical number of odorants p_{max} , scales linearly with N , the number of representatives of a single odorant, M , has to grow at least as fast as N^2 . This ensures that increasing M further does not change the results of the calculation (e.g. the value of p_{max}) and hence the M discrete points indeed represent correctly the continuous curves on which they lie.

Our problem has been turned into one of learning $M(p+1)$ “patterns”, that constitute our training set \mathcal{L} . For technical reasons it is convenient to introduce and work with normalized patterns,

$$\xi^{\mu\zeta} = \frac{\mathbf{S}^{\mu\zeta} s^{\mu\zeta}}{\sqrt{(\mathbf{S}^{\mu\zeta})^2}} \quad (9)$$

with $\zeta = 1, \dots, M$ running over the M discrete concentrations and $\mu = 0, 1, \dots, p$ over all odorants. Note that we also multiplied each pattern $\mathbf{S}^{\mu\zeta}$ by its desired output, $s^{\mu\zeta}$; after this change of representation the condition of linear separability (8) becomes

$$\text{sign}(\mathbf{w} \cdot \xi^{\mu\zeta}) > 0 \quad \text{for } \mu = 0, 1, \dots, p \text{ and } \zeta = 1, 2, \dots, M \quad (10)$$

B. The Learning algorithm

The question posed above, whether the target odorant can or cannot be distinguished from the background, has been reduced to the following one: is there a set of weights w_i , $i = 1, \dots, N$, for which all $M(p+1)$ inequalities (10) are satisfied? This problem is of the type studied by Rosenblatt [8], and is an example of classification by a single layer perceptron. A solution exists if one can find a weight vector \mathbf{w}^* (that parametrizes the perceptron) such that for all the patterns $\xi^{\mu\zeta}$ in the training set \mathcal{L} the “field”

$$h^{\mu\zeta} = \xi^{\mu\zeta} \cdot \mathbf{w}^* > 0, \quad (11)$$

i.e. the projection of the weight vector \mathbf{w}^* onto all patterns $\xi^{\mu\zeta}$ is positive. We wish to determine the size of the training set \mathcal{L} , i.e. the number of background odorants p , for which a solution \mathbf{w}^* can be found. This is done by executing a search for a solution \mathbf{w}^* by means of a *learning algorithm*. There are several learning algorithms (e.g. Rosenblatt [8], Abbott and Kepler [9]) in the literature; all are guaranteed to find such a weight vector, in a finite number of steps, *provided a solution exists*. If, however, the problem is *not LS* and a solution *does not exist*, most learning algorithms will just run ad infinitum. An exception to this is the algorithm of Nabutovsky and Domany (ND) [5] which detects, in finite time, that a problem is non-learnable. This is a batch perceptron learning algorithm,

presenting sequentially the entire training set \mathcal{L} in one “sweep” and repeating the process until either a solution is found or non-learnability is established. We found that this algorithm is efficient and convenient to use (see [9] for other algorithms that detect non-**LS** problems). ¹.

ND introduced a parameter d which they called *despair*, which is calculated “on line” in the course of the learning process. d is bounded if the training set \mathcal{L} is **LS**. Since the ND algorithm can be shown to either find a solution \mathbf{w}^* , or transgress the bound for d in a finite number of learning iterations, d effectively signals if the learning set \mathcal{L} fails to be linearly separable. The theorem they proved can be easily extended to the distribution of examples in our problem ². We introduced a halting criterion, which is probably more stringent than necessary, since no attempt has been made to determine an optimal lower bound. In figures 2a and 2b typical evolutions of the despair are shown for an **LS** case and for a non-**LS** case, respectively. The behavior of d is strikingly different in the two cases, showing that indeed d is a good indicator of learnability. In the learnable cases d grows linearly with the number of learning sweeps until a solution is found (and the curves terminate). In the non-**LS** cases d grows exponentially with the number of sweeps and would continue to grow; the process is halted when its value exceeds a known bound, that must be satisfied if the problem is **LS**.

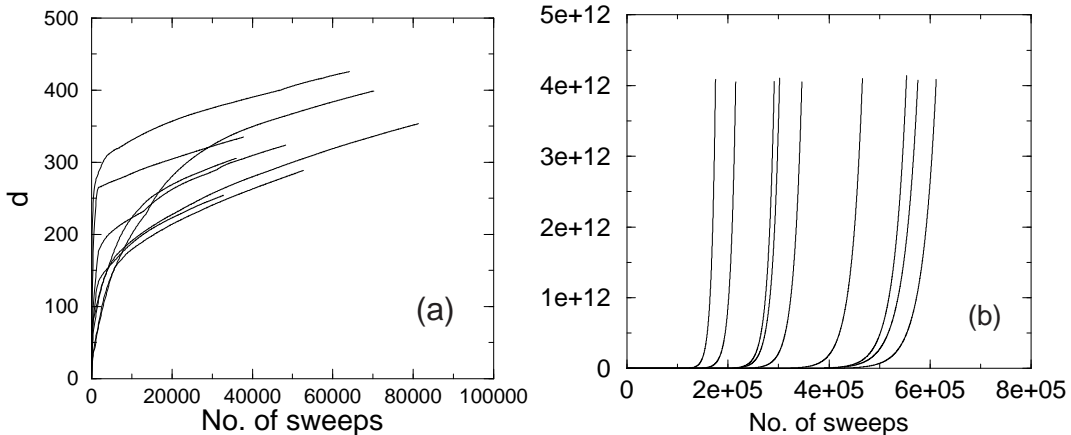


FIG. 2. Despair d as a function of the number of sweeps for $N = 10$, $H_{max} = 50$, $H_{min} = 0.5$ and $p = 25$; learnable cases are shown in (a) while those that were not learnable are shown in (b). Note the huge difference in both vertical and horizontal scales.

We now describe the ND algorithm used in the simulations. The patterns of the learning set \mathcal{L} are presented one at a time (one cycle constitutes a sweep). ND have shown [5] that for binary valued patterns ($\xi_i = \pm 1$), i.e. patterns on vertices of a unit hypercube, an upper bound d_c exists iff the training set is **LS**. On the other hand the dynamics is shown to take d beyond that bound in a finite (linear in N) number of iterations unless a solution exists and the algorithm halts. Initialize the process with $d = 1$, $\mathbf{w} = \xi^1$. Go to the next example. If it is correctly classified, do nothing to the current weight vector and go to the next example. Once a misclassified example $\xi^{\mu\zeta}$ is found, update the weight vector as well as the parameter d , according to

$$\mathbf{w}_{\text{new}} = \frac{\mathbf{w} + \eta \xi^{\mu\zeta}}{|\mathbf{w} + \eta \xi^{\mu\zeta}|} \quad (12)$$

$$d_{\text{new}} = \frac{d + \eta}{\sqrt{1 + 2\eta h^{\mu\zeta} + \eta^2}} \quad (13)$$

η is not just a learning rate parameter but an effective modulation function, chosen in order to maximize the increase of the despair as

¹The fact that we use a learning procedure to establish the boundaries of linear separability doesn't imply and is unrelated to any possible plasticity of the olfactory bulb. The algorithm is being used only to either find a solution or show that it doesn't exist.

²The original ND algorithm was designed for binary vectors, i.e. pointing at the corners of a N -dimensional hypercube. It can be shown that the theorem can be extended to vectors on the unit sphere.

$$\eta = \frac{1/d - h^{\mu\zeta}}{(1 - h^{\mu\zeta}/d)} \quad (14)$$

The learning dynamics halts if all patterns are correctly classified or alternatively, if the value of d exceeds an upper bound, given by

$$d > d_c = \frac{N^{(N+1)/2}}{2^{N-1}} \quad (15)$$

This is guaranteed to happen in at most $N d_c^2$ steps.

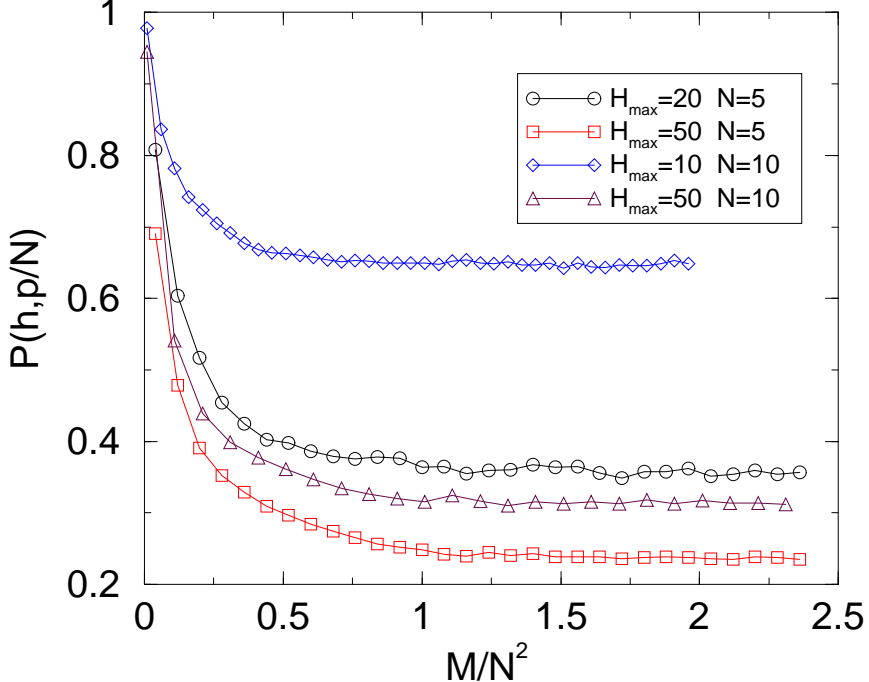


FIG. 3. The estimated probabilities saturate when M , the number of representatives of a given odorant, exceeds $M_c \approx N^2$. For brevity we denote $P(H_{min}, H_{max}, p, N)$ by $P(h, p/N)$. In all cases $p = 25$ odorants were used with $H_{min} = 0.5$.

III. NUMERICAL EXPERIMENTS

Since there is a large number of parameters that are to be varied, we present first a detailed description of the manner in which we deal with every one of them.

There are two random elements in our studies. The first is in the selection of M concentrations for each odorant, within the range (1); the second is the choice of K_i^μ , the affinity of receptor i to odorant μ , selected at random from the distribution $\tilde{\psi}(K)$ of eq. (2). For every choice of the remaining variables we generate an ensemble of experiments and average the object we are measuring over these two random elements. We select L_a times the set of affinities and for each of these perform L_c times the random selection of concentrations.

The object we wish to estimate numerically is the probability P , that the p curves described in the Introduction are **LS**. To this end we place M points on each curve and measure the corresponding probability $P(H_{min}, H_{max}, p, N; M)$. As we will see, for large enough values, $M > M_c$, this probability becomes independent of M ; beyond M_c the set of M discrete points represents the corresponding curves faithfully and hence the limiting value $P(H_{min}, H_{max}, p, N; M > M_c)$ is our estimate for $P(H_{min}, H_{max}, p, N)$.

Finally, we are interested in this function in the large N limit, i.e. when $N \rightarrow \infty$ and $p \rightarrow \infty$, while $\alpha = p/N$ is fixed. This limit is obtained by extrapolating our finite N results, using finite size scaling methods.

Our first task is to determine how M_c scales with N ; that is, how dense a set of concentrations is to be used so that M discrete points represent accurately the continuous curves $S_i^\mu(H^\mu)$ of eq. (4)?

A. Scaling of M_c

We choose values for N (number of receptor cells), p (number of odorants) and H_{min}, H_{max} (limiting concentrations). We also set some value for M , the number of concentrations by which every odorant is represented (M will be varied).

We proceeded according to the following steps:

1. Draw from the distribution $\tilde{\psi}(K)$ a set of affinities K_i^μ for all N receptors and p odorants.
2. Generate for each odorant M concentration values, from a uniform distribution in the allowed range $H_{min} < H < H_{max}$ and construct the set $\{\xi^{\mu\zeta}\}$ of normalized patterns.
3. Run the ND learning algorithm until it stops; register whether the set $\{\xi^{\mu\zeta}\}$ was **LS** or not.

Steps 2,3 are repeated L_c times for each set of affinities; the whole process 1 - 3 is repeated for L_a different sets of affinities. We used $L_a = 100$; increasing it further made no difference. With such a value of L_a the results did not depend on L_c ; having tried $1 \leq L_c \leq 10$ we used $L_c = 1$ in our simulations.

At this point we have $L_c \cdot L_a$ experiments, out of which a fraction of $P(H_{min}, H_{max}, p, N, M)$ cases were linearly separable. Keeping H_{min}, H_{max}, p, N fixed, we increase M and repeat the entire process, obtaining the probability functions $P(H_{min}, H_{max}, p, N, M)$, that are plotted in Fig. 3 versus M/N^2 . Clearly the curves saturate when $M > M_c \approx N^2$. From this point on we have fixed the value of M at $M = N^2$. This numerical result can be estimated by using the analysis of Gardner and Derrida [4] for the capacity of biased patterns, using for the “magnetization” m the value $m \propto 1/N$. This gives, in addition to the leading behavior $M_c \approx N^2$, logarithmic corrections as well. We cannot rule out the possibility of such logarithmic corrections to the scaling we found here.

B. Measuring the probabilities $P(H_{max}, p, N)$

In all our experiments we fixed the value of $H_{min} = 0.5$ and hence the dependence of the probability on this variable has been suppressed. For various values of N , p and H_{max} we calculate $P(H_{max}, p, N)$ in the manner described above. Keeping N and H_{max} fixed, we increase p . For $p \ll N$ we have $P(H_{max}, p, N) \approx 1$ and the probability of **LS** decreases as p increases. We stop increasing p when $P(H_{max}, p, N)$ becomes smaller than some ε .

The variation of $P(H_{max}, p, N)$ vs p/N is presented, for three values of H_{max} and four values of N , in Fig. 4. The results presented in these figures are discussed in the next subsection.

We should mention here that for large N we used a heuristic modification of the ND halting criterion, to label a problem as non-**LS**. Typical evolutions of the despair parameter are shown in figures 2. Each curve represents the history for a single learning set. Notice the huge difference in scales for the learnable and the unlearnable cases. The wide separation in final values of d suggests that a more practical, e.g. smaller, upper bound be used. For $N = 30$ (the largest value treated here) we used a different halting criterion in order to escape from the need to reach an exponentially high upper bound. After a small number of successful trial runs (that did produce linear separability) we identified the highest value of the despair d_m that was reached for a learnable set. This value was used to define our new heuristic halting criterion, $d_{bound} = N d_m$.

C. Finite Size Scaling Analysis

As expected, for small $\alpha = p/N$ the probability for linear separability is close to 1, and it decreases as α increases. The curves obtained for fixed H_{max} become sharper as N increases.

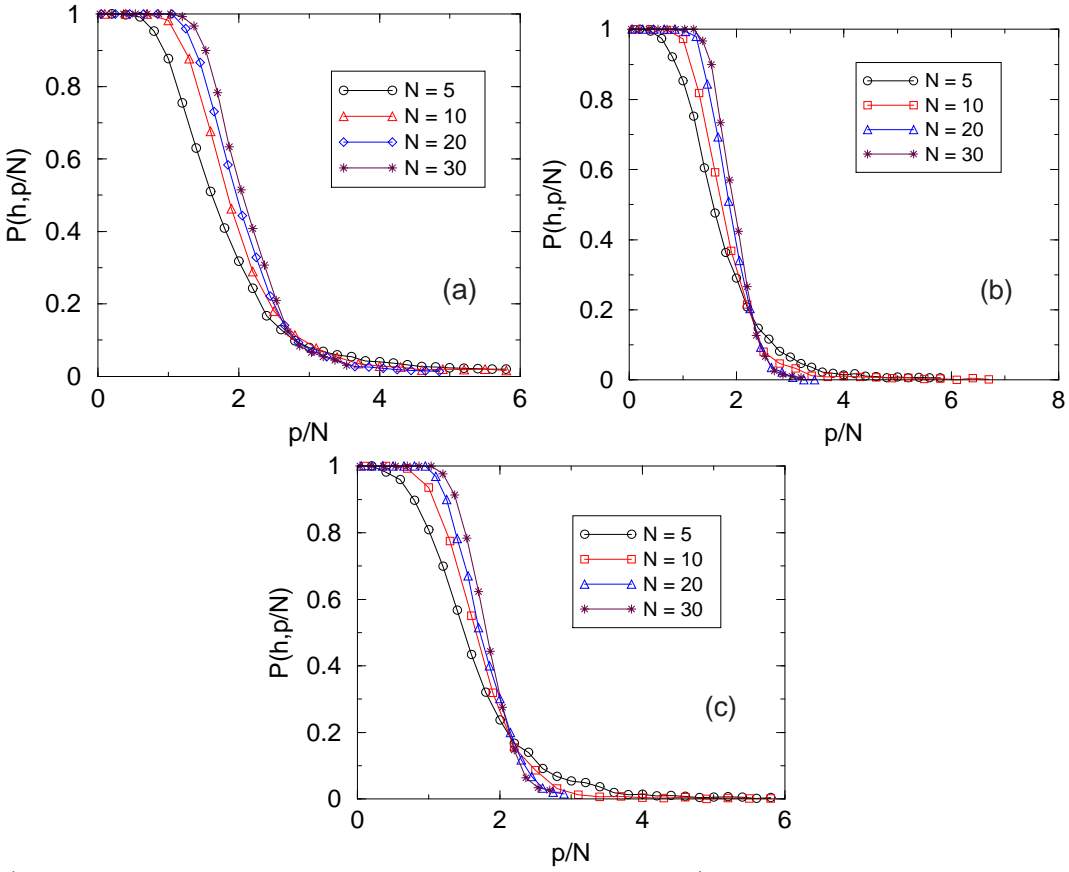


FIG. 4. (a) Probability that a learning set is LS as a function of $\alpha = p/N$, for maximal concentration $H_{max} = 50$ and $H_{min} = 0.5$ (b) $H_{max} = 70$ and $H_{min} = 0.5$ (c) $H_{max} = 100$ and $H_{min} = 0.5$

Note that curves obtained for different N values cross at approximately the same value of α . Similar behavior of the corresponding probability functions has been observed for random uncorrelated patterns [10]. Notice, however, that the crossing point is at some probability $P < 1/2$. Similar curves, obtained for other architectures, such as the parity and committee machines [7] crossed at $P > 1/2$. If there is a sharp transition in the thermodynamic limit ($N \rightarrow \infty$), these curves should approach a step-function, with

$$P(H_{min}, H_{max}, \alpha) = \begin{cases} 1 & \text{if } \alpha < \alpha_c(H_{min}, H_{max}) \\ 0 & \text{otherwise} \end{cases} \quad (16)$$

That is, for α below a certain $\alpha_c(H_{min}, H_{max})$, a learning set will be **LS** with probability one and conversely, it will be **LS** with probability zero for $\alpha > \alpha_c(H_{min}, H_{max})$. The manner in which such a step function is approached as $N \rightarrow \infty$ can be described by a finite size scaling analysis (e.g. [6]).

For each value of H_{max} (keeping H_{min} fixed) we tried a simple rescaling of the α variable, with two adjustable parameters, α_c and ν ;

$$y = (\alpha - \alpha_c)N^{\frac{1}{\nu}}.$$

For the proper choice of α_c and ν we expect *data collapse*; that is, curves obtained for different values of N are expected to fall onto a single function, provided $P(H_{max}, \alpha, N)$ is plotted versus the scaled variable y . As can be seen on Figures 5a,b and c, this expectation is borne out; the evidently good data collapse indeed substantiates the idea of a sharp transition at α_c . As N increases, the function $P(H_{max}, \alpha, N)$ becomes increasingly sharper; its width near α_c decreases at a rate governed by the exponent ν .

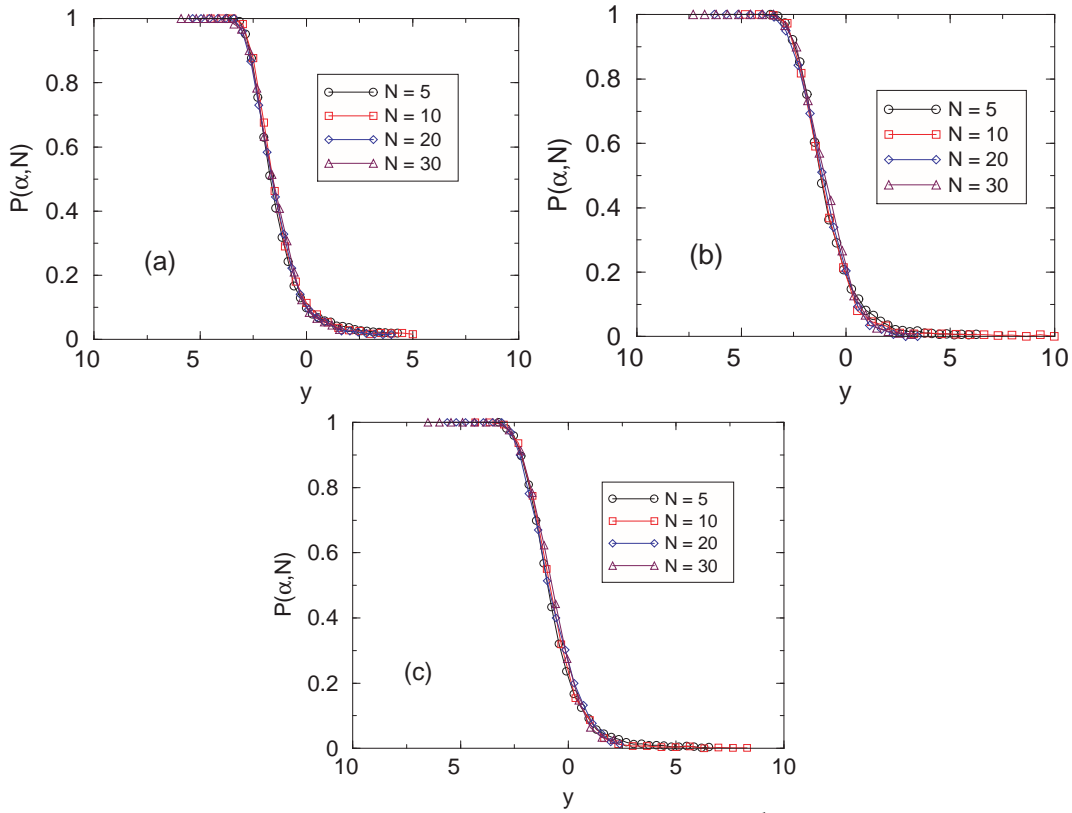


FIG. 5. (a) Probability that a learning set is LS as a function of $y = (\alpha - \alpha_c)N^{\frac{1}{\nu}}$, for maximum concentration $H_{max} = 50$ and $H_{min} = 0.5$ (b) $H_{max} = 70$ and $H_{min} = 0.5$ (c) $H_{max} = 100$ and $H_{min} = 0.5$ The result of a least squares fit are (a) $H_{max} = 50, \nu = 4.8, \alpha_c = 2.8$, (b) $H_{max} = 70, \nu = 2.85, \alpha_c = 2.25$ (c) $H_{max} = 100, \nu = 2.75, \alpha_c = 2.1$

Finally, we present in figure 6 the behavior of α_c as a function of H_{max} (for fixed H_{min}). As H_{max} increases, separation of the curves becomes an increasingly difficult task and hence $\alpha_c(H_{max})$ decreases. We find that it saturates at a low value close to $\alpha_{min} = 2$, which is exactly the Cover result. This interesting point is explained in the Appendix.

Note that even though we deal here with linear separability of *curves*, which one would expect to be a more difficult task than separating points, we found that our α_c exceeds the value derived for points, $\alpha_c = 2$. The reason is that this is the critical capacity for separating *random, independent* points; the curves we are trying to separate are *not independent of each other*. In fact by construction we have $S_i^\mu > 0$ for all the background odorants; hence all these curves lie on one side of an entire family of planes. The target odorant, which also satisfies $S_i > 0$, should lie on the other side of the separating plane.

The curve $\alpha_c(H_{max})$ is, in effect, a *phase boundary*; on one side we have a “phase” in which the problem is **LS**, while on the other (high α) region it is not. We present now a brief description of the manner in which linear separability breaks down as we cross this phase boundary by increasing H_{max} at fixed α .

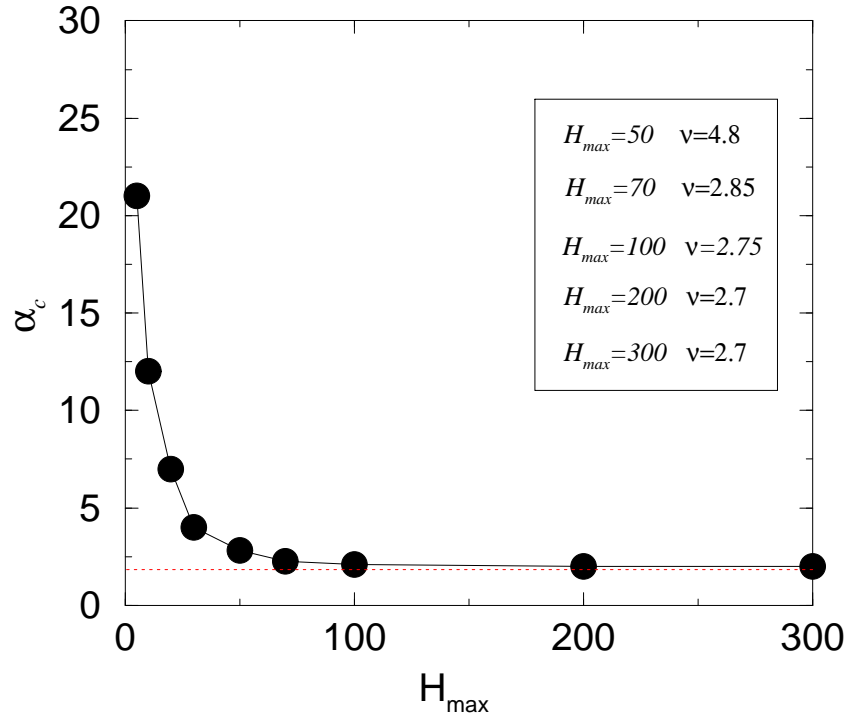


FIG. 6. Phase diagram in the α, H_{max} plane for $H_{min} = 0.5$. The curve separates the α, H_{max} plane into the regions where the network can distinguish the target odorant (below), and where it cannot (above). Below(Above) the curve a learning set is(not) **LS** with probability one in the thermodynamic limit. The horizontal dotted line is $\alpha_{th} = 2$.

D. Breakdown of LS near phase boundary

The manner in which **LS** breaks down as H_{max} increases beyond the phase boundary is nicely illustrated by the set of figures 7 and 8.

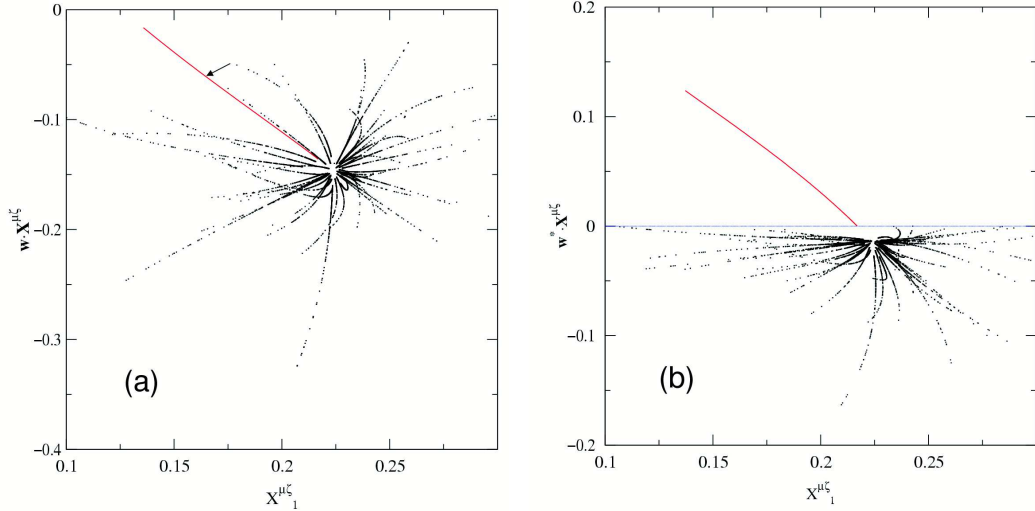


FIG. 7. The curves representing the p background odorants and the target odorant (marked by an arrow), in a **LS** case, $\alpha < \alpha_c$, for $H_{max} = 50, H_{min} = 0.5, N = 20$. In figure (a) the curves are projected onto a randomly selected plane; in (b) onto a plane Q (see text), that contains the weight vector \mathbf{w}^* , determined by the learning algorithm. The horizontal dotted line in figure (b) demonstrates linear separability of the target from background.

Consider the p curves, in an N -dimensional space, which represent the odorants, in a linearly separable case. We present in figure 7(a) a projection of these curves onto a randomly chosen plane. One of these (indicated by an arrow)

is the target odorant; it seems to be entangled with the other curves. The point at which all curves seem to converge corresponds to the maximal concentration.

The purpose of the learning dynamics is to find a particular direction \mathbf{w} , along which one is able to separate the target curve from the others. Denote by \mathcal{V} the hyperplane that passes through the origin and is *perpendicular* to \mathbf{w} ; this is the linear manifold that separates the target from all the background curves. Select now any plane \mathcal{Q} , that contains \mathbf{w} , and project all curves onto \mathcal{Q} ; this produces Fig. 7(b). The horizontal dotted line shown here is the intersection of the hyperplane \mathcal{V} with the plane \mathcal{Q} . The projected background odorant curves lie on one side of this line and the target on the other. The situation depicted here is **LS**.

Consider now what happens when we turn the problem into non - **LS** by increasing H_{max} beyond the phase boundary. As we increase the maximal concentration, the target odorant's curve penetrates to the "wrong" side of the hyperplane \mathcal{V} . A picture of this situation is shown in Fig. 8(a).

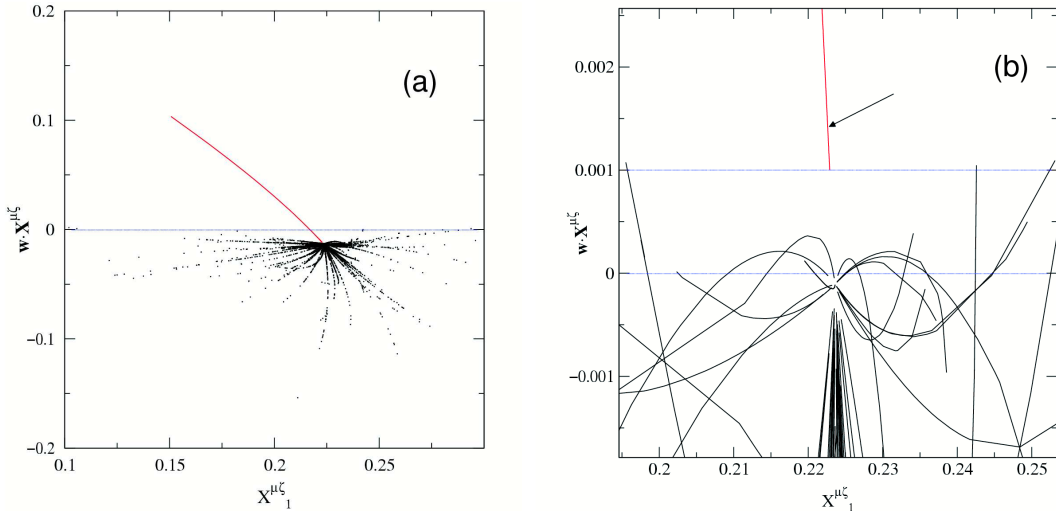


FIG. 8. The same situation as in Fig. 7, but with H_{max} increased beyond the limit of learnability. (a) Projecting the curves onto the same plane as for the **LS** case, we see that the target penetrates to the "wrong" side of the broken line. (b) Further attempts to learn new \mathbf{w} will fail.

This is a non **LS** problem - which means that no matter how long we run our learning algorithm, we will never find a hyperplane \mathcal{V} that separates the target from all the background. If nevertheless we keep running our learning algorithm, the direction of our candidate for \mathbf{w} will keep changing as we "learn", but since the critical capacity curve of figure 6 has been crossed, no amount of further learning will produce a separating plane. The density of points near the high concentration limit is much larger than for low concentrations. Hence further learning will perhaps be able to separate the target from the background at high concentrations - but then separability breaks down at low concentrations (see Fig. 8(b)).

IV. SUMMARY AND DISCUSSION

In the olfactory bulb of most vertebrates, each secondary neuron (mitral or tufted cell) receives input from only one glomerulus, which in turn is innervated, in all likelihood, by axons stemming from olfactory epithelial sensory cells that all express the same olfactory receptor protein. Thus, the grandmother cell modeled here may not simply represent a mitral or tufted cell. However, when the network of periglomerular and granule cells (interneurons) is taken into account, then it is fair to state that each mitral cell receives (indirect) input from a large number of different olfactory receptor types. Thus, the present analysis may be relevant to the kind of neuronal processing that takes place in the first neuronal relay station of the olfactory pathway, the olfactory bulb. Alternatively, it may represent, in abstract fashion, information processing that takes place both in the olfactory bulb and at higher olfactory central nervous system centers.

Previously, several studies have been published that analyze neuronal networks for the olfactory System [13] [14] [16] [15] [17] [18]. However, none of these was based on a quantitative model for the affinity relationships within the entire olfactory receptor repertoire. Here, we use the Receptor Affinity Distribution (RAD) model, which was developed, based on general biochemical considerations, for receptor repertoires, including that of olfactory receptors. The power

of this approach is in utilizing a global knowledge about the repertoire to analyze the fidelity of discrimination among odorants. It has been pointed out in the past, that the RAD model may be used to analyze the signal to noise ratio in systems in which specific binding to a receptor has to be distinguished from the background of numerous other receptors which constitute "non-specific binding" [1] [12]. Here, we apply a similar concept to an analysis of signal to noise discrimination in the case of a neuronal network whose input stems from a receptor repertoire.

The results presented here suggest that for a fixed number of background odorants there is a maximal odorant concentration beyond which odorant discrimination becomes impossible. This is not surprising, since olfactory receptors are saturable, and at very high concentrations weak affinity receptors as well as high affinity ones will generate comparable signals. However, it is noteworthy that despite the fact that information capacity for odorant discrimination rapidly declines as odorant concentration goes up, the presently analyzed network is still capable of discrimination even at concentrations for which $H\langle K \rangle$ is of the order of a few hundred (where $\langle K \rangle$ is the average affinity).

The model network consists of N sensory neurons, each of which is characterized by a set of affinities to a number of odorants. When any particular odorant, μ , is present, sensory neuron i produces a (nonlinear) response, S_i^μ . These responses constitute the inputs to a single processing unit (secondary neuron), which performs weighted summation of all the N inputs. The secondary neuron's output is the sign of this weighted sum. The aim of this single processing unit is to identify *one single odorant* separate it from all the others that may be sensed by the system. This secondary neuron plays the role of a "grandmother cell" for a particular target odorant. An assembly of P_0 such secondary neurons may constitute, together with the sensory neurons, a system that is able to clearly identify the presence of P_0 target odorants, from a background of P odorants.

We posed a well defined quantitative question: given that each odorant may appear with a concentration H_μ that lies in a certain range, $H_{min} < H^\mu < H_{max}$, what is the maximal number of background odorants $P_c = \alpha_c N$, from which a single target can be separated with probability 1? The answer is summarized in Fig. 5, where α_c , the critical capacity, is plotted vs. H_{max} . The result is obtained in the limit of large N (i.e. many sensory neurons - in fact, for $N = 100$ this result should already give excellent precision). For a dynamic range of H_{max}/H_{min} of about 100 we find $\alpha_c \approx 2.5$. That is, for say $N = 300$ sensory neurons we can distinguish the target from about 750 background odorants. Hence if we assemble 750 odorants and appoint a grandmother cell for each, we will be able to identify them one by one.

In order to get this quantitative answer we had to generalize an old problem, of *Linear Separability* of P points on an $N - 1$ dimensional hypersphere, to the new problem of linearly separating P curves that lie on the same hypersphere. We have shown that in order to represent a curve by discrete points that lie on it, we have to place $M \propto N^2$ points on each curve. The results were obtained by a perceptron learning algorithm that signals when a problem is *unlearnable*, i.e. non-linearly-separable.

Results obtained at various values of N were shown to collapse when plotted as functions of properly defined scaled variables, which allowed easy extrapolation to large values of N .

APPENDIX

The behavior of the phase boundary for large concentrations $\alpha_c \rightarrow 2$ (figure 5) is quite surprising since the network may be expected to enter a totally confused state due to the saturation of the nonlinear sensory neurons. This could be expected to lead instead to $\alpha_c \rightarrow 0$. That the Cover result ($\alpha_c = 2$) is recovered in the high concentration regime can be in fact be understood by the following argument.

We first calculate the probability $P(S)$, that a sensory unit gives a response S to the presentation of an odorant in the range (1), by

$$P(S) = \langle \delta(S - f(HK)) \rangle \quad (17)$$

where the average is taken over possible concentrations H uniformly distributed in range (1) and according to the RAD model, over the affinities, $\tilde{\psi}(K)$ of equation (2). f is given by equation (6). The integrals lead to

$$P(S) = \frac{\sqrt{\pi} (1 - S)^{-2}}{\sigma (H_{max} - H_{min})} \left(\text{Erfc} \left(\frac{S}{\sigma H_{max} (1 - S)} \right) - \text{Erfc} \left(\frac{S}{\sigma H_{min} (1 - S)} \right) \right), \quad (18)$$

where $\text{Erfc}(x) = \int_0^x \exp(-u^2) du / \sqrt{\pi}$ is the complementary error function. This probability has one peak which sharpens and moves to higher values of S as H_{max} grows. However at the very ends of the interval, $S = 1$ or 0, the probability is zero. That $P(1) = 0$ for every H_{max} is the source of the surprise. The peak which concentrates all

the probability , gets arbitrarily close to $S = 1$, as the concentration increases, but never makes it to the extreme of the interval. In fact $S_{peak} \approx 1 - c/H_{max}$. Therefore the components of the vectors $\mathbf{S}^{\mu\zeta}$ will be with overwhelming probability at the peak position, which can be written as $S_i^\mu = 1 - \varepsilon_i^\mu$ with all $\varepsilon_i^\mu(H_{max}, K_i^\mu)$ small but strictly positive. Neglecting second order terms in ε the normalized patterns will then be:

$$\begin{aligned}\tilde{S}_i^\mu &\equiv \frac{S_i^\mu}{|\mathbf{S}^\mu|} = \frac{(1 - \varepsilon_i^\mu)}{\sqrt{N} (1 - 2\bar{\varepsilon}^\mu)^{\frac{1}{2}}} \\ &= (1 - \varepsilon_i^\mu + \bar{\varepsilon}^\mu) / \sqrt{N}\end{aligned}$$

Therefore the $\tilde{\mathbf{S}}^{\mu\zeta}$ vectors are unbiasedly distributed around $(1, 1, \dots, 1) / \sqrt{N}$. We are taken back to the original Cover-Gardner problem of separating p unbiased patterns with a hyperplane and the result $\alpha_c = 2$ is no longer a surprise. This argument doesn't deal with the asymptotic behavior of the capacity in the presence of any kind of noise. In that case the naive expectations that $\alpha_c \rightarrow 0$ for $H_{max} \rightarrow \infty$ are probably borne out.

Acknowledgements We thank Ido Kanter for most useful discussions. The research of ED was supported by the Germany-Israel Science Foundation (GIF), the Minerva Foundation and the US-Israel Binational Science Foundation (BSF). The work reported here was initiated during visits of NC to the Weizmann Institute, that were supported by grants from the São Paulo Society of Friends of the Weizmann Institute and by the Gorodesky Foundation. JEPT's research was supported by a graduate fellowship of the Fundação de Amparo à Pesquisa do Estado de São Paulo (Fapesp). NC received partial support from the Conselho Nacional de Desenvolvimento Científico e Tecnológico (CNPq)

- [1] D. Lancet, E. Sadovsky and E. Seidman, Proc. Natl. Acad. Sci. USA, **90** 3715 (1993)
- [2] L Schläfli, Theorie der vielfachen Kontinuität, Gesammelte Matematische Abhandlungen, ed. Steiner-Schläfli-Komitee Basel, Birkhäuser p171 (1852) *apud* W Kinzel *Phil. Mag.* **B 77**, 1455 (1998)
- [3] E Gardner, J. Phys. A **21**, 257 (1988)
- [4] E. Gardner and B. Derrida, J. Phys. A **21**, 271 (1988)
- [5] D. Nabutovsky and E. Domany, Neural Computation, **3**, 604 (1991)
- [6] e.g. V. Privman, Ed. *Finite-size Scaling and Numerical Simulations of Statistical Systems*, World Scientific, Singapore, 1990
- [7] W. Nadler and W. Fink, Phys. Rev. Lett. **78**, 555 (1997)
- [8] F. Rosenblatt, *Principles of Neurodynamics*, Spartan Books, New York (1962)
- [9] L. F. Abbott and T. B. Kepler J. Phys. A. **22**, L711 (1989)
- [10] T. Cover, IEEE Tran. Elect. Comput., **14**, 326 (1965)
- [11] Minsky and Papert *Perceptrons* MIT Press, Cambridge, MA (1969)
- [12] D. Lancet, A Horovitz and E Katchalski-Katzir Molecular recognition in biology: Models for analysis of protein-ligand interactions. Behr, J.P., ed., John Wiley and Sons Ltd., pp. 25-71 (1994)
- [13] W. Freeman, <http://sulcus.berkeley.edu/FLM/MS/WJFMM.html>
- [14] J. Hopfield *Proceedings of the Nat. Acad. Sci. USA* **88** 6462 (1991)
- [15] M. A. Wilson and J. M. Bower *J. Neurophysiol* **67** 981 (1992)
- [16] Z. Li an J. Hopfield *Biol. Cybern* **61** 379 (1989)
- [17] Z. Li *Biol. Cybern* **62** 349 (1990) and Modeling the Sensory Computations of the Olfactory Bulb Published in Models of Neural Networks Vol. 2, Eds. J. L. van Hemmen, E. Domany, and K. Schulten, Springer-Verlag New York, (1995)
- [18] Z. Li and J. Hertz *Network: Computation in Neural Systems* **11**. 83 (2000)